

# The 3D transport diagram of a triple quantum dot

G. Granger,<sup>1,\*</sup> L. Gaudreau,<sup>1,2</sup> A. Kam,<sup>1</sup> M. Pioro-Ladrière,<sup>2</sup>  
S.A. Studenikin,<sup>1</sup> Z.R. Wasilewski,<sup>1</sup> P. Zawadzki,<sup>1</sup> and A.S. Sachrajda<sup>1</sup>

<sup>1</sup>*Institute for Microstructural Sciences, National Research Council Canada, Ottawa, ON Canada K1A 0R6*

<sup>2</sup>*Département de physique, Université de Sherbrooke, Sherbrooke, QC Canada J1K 2R1*

We measure a triple quantum dot in the regime where three addition lines, corresponding to the addition of an electron to each of three dots, pass through each other. In particular, we probe the interplay between transport and the tridimensional nature of the stability diagram. We choose the regime most pertinent for spin qubit applications. We find that at low bias transport through the triple quantum dot circuit is only possible at six quadruple point locations. The results are consistent with an equivalent circuit model.

PACS numbers: 73.63.Kv, 73.23.-b, 73.23.Hk

Double quantum dots have been extensively studied and utilized in quantum information spin qubit experiments.<sup>1-3</sup> Recently we have presented a highly tunable TQD layout<sup>4</sup> aimed at quantum information applications, where the stability diagram was mapped out using standard charge detection techniques. The experimental realization of this type of tunable TQD is important, as it provides a platform for testing a variety of predicted novel quantum information functionalities and running simple algorithms.<sup>5-12</sup>

Electron transport in double quantum dot systems is limited to the neighborhood of special locations in the stability diagram where three electronic configurations are degenerate (triple points).<sup>1</sup> In this paper we probe the equivalent transport conditions in triple quantum dots (TQDs). While the stability diagram of a TQD circuit has been studied in detail using conventional charge detection techniques<sup>4,13-15</sup> and certain transport features have been observed in these experiments,<sup>14-16</sup> in this paper we reveal the full interplay between the stability diagram and the conditions for electron transport.

We first use a charge detector<sup>17</sup> to set up specific electronic configurations. We focus mainly on the regime between (1,0,1) and (2,1,2), which is the most relevant for spin qubit applications. The 3D nature of the stability diagram and transport regimes is studied by tuning plunger gate voltages which control the occupation numbers of the three individual dots. We compare our results to an equivalent circuit model.<sup>13,15</sup>

Details describing of the device have been published elsewhere.<sup>4</sup> Samples are bias-cooled with 0.25 V on all gates on a dilution refrigerator. The electron temperature is  $\approx 110$  mK. We use standard low current AC and DC techniques for both transport and charge detection (using the left QPC) measurements. The bias across the QPC is  $V_{\text{QPC}}=0.2$  mV for the charge detection measurements unless indicated otherwise. For transport, a bias of  $V_{\text{ds}}=0.1$  mV is applied across the TQD device.

Figures 1(b) and (c) contain transconductance data from two TQD devices in the few-electron regime. The relevant regime for charge qubits<sup>5</sup> is shown in Fig. 1(b) and that for spin qubits,<sup>6,18</sup> in Fig. 1(c). These electronic

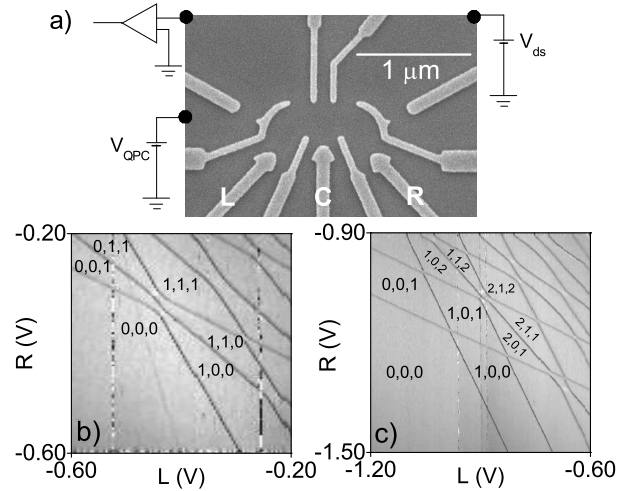


FIG. 1: (a) Electron micrograph of a device similar to the ones measured. The plunger gate for the left, center, and right dots are labeled L, C, and R, respectively. Black dots represent Ohmic contacts.  $V_{\text{ds}}$  is the drain-source bias across the TQD, and  $V_{\text{QPC}}$  is the bias across the QPC. The current preamplifier is shown schematically. (b) and (c) Charge detection transconductance measurements in the L-R space, at  $V_{\text{ds}}=0$  mV plotted with a greyscale where black is low and white is high. (b) The absolute electronic configurations from (0,0,0) to (1,1,1) are indicated.  $V_{\text{QPC}}=0.3$  mV (c) The electronic configurations from (0,0,0) to (2,1,2) are indicated.

configurations can be achieved in both the devices that have been measured (not shown).

Figure 2 shows the evolution of the 3D stability diagram as a function of C, the voltage on the central plunger gate. The electronic configurations ( $N_L, N_C, N_R$ ) are identified by counting from the (0,0,0) configuration shown in Fig. 1(c).

The region of interest in Fig. 2 is the regime where three addition lines cross between (1,0,1) and (2,1,2). Depending on the value of C, the size of the stability diagram regions with electronic configurations (1,1,1) and (2,0,2) can be tuned continuously from no (1,1,1) region

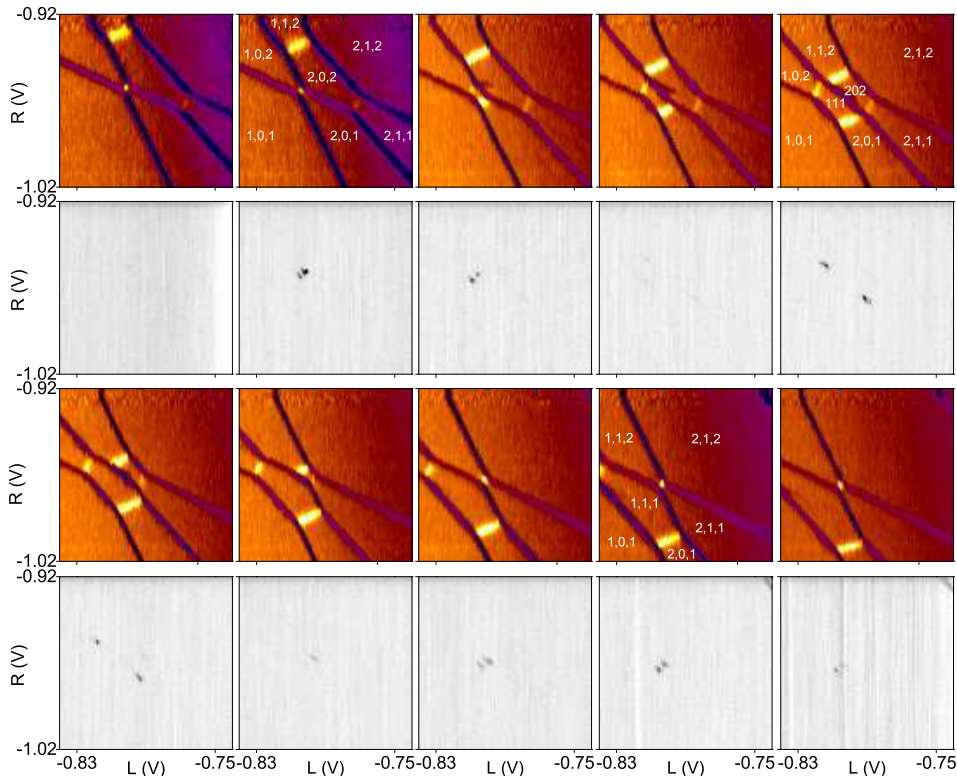


FIG. 2: (Color online.) Charge detection and transport diagrams in the L-R voltage space as a function of gate voltage  $C$ . The values of  $C$  in the upper two rows go from  $-0.224$  V to  $-0.216$  V, while they go from  $-0.214$  V to  $-0.206$  V in the lower two rows. The charge detection transconductance data at  $V_{ds}=0$  mV (1<sup>st</sup> and 3<sup>rd</sup> rows) are plotted with an arbitrary unit colorscale (dark blue is low transconductance, orange is medium, and yellow is high). The transport data (2<sup>nd</sup> and 4<sup>th</sup> rows) are taken with  $V_{ds}=0.1$  mV across the TQD. The greyscale from white to black corresponds to a current range of 370 fA through the TQD. The electronic configurations are indicated on the charge detection plots for  $C=-0.222$ ,  $-0.216$ ,  $-0.208$  V, where clear black spots in the respective transport plots are observed.

and a large  $(2,0,2)$  region to a large  $(1,1,1)$  region and no  $(2,0,2)$  region. A symmetric case where the  $(1,1,1)$  and  $(2,0,2)$  regions are approximately the same size is also observed. The latter regime is important when considering transport.

The bright lines in Fig. 2 correspond to charge transfer lines between dots that do not involve any changes in the total number of electrons. The boundary between  $(1,1,1)$  and  $(2,0,2)$  is an example of a charge reconfiguration (commonly referred to as a QCA event due to its similarity to Quantum Cellular Automata<sup>13</sup>) at which every dot changes its electron occupation as the total number of electrons changes by one.<sup>19</sup>

We now turn to examining the transport through the TQD. The DC current measurements in Fig. 2 are shown as a function of the  $C$  gate voltage, and each transport diagram can be compared to the charge detection stability diagram in the row immediately above it. As the voltage on  $C$  progressively increases, two closely spaced current spots first appear and disappear, then two well separated current spots appear and disappear, and two additional closely spaced current spots appear and disappear. The total number of current spots is six.

The simultaneous appearance of pairs of current spots is interesting. We focus on the first two current spots from Fig. 2, which we label QPs 1 and 2. Figure 3 contains their  $C$  gate dependence.<sup>20</sup> The data in Fig. 3 are taken with a slightly higher resolution than in Fig. 2, so the current spots now appear as roughly triangular re-

gions. As  $C$  is made less negative, the current intensity of the two triangles changes so that QP 2 gets progressively replaced by QP 1.

For clarity we reproduce in Fig. 4 the charge detection and transport data from Fig. 2 where clear pairs of transport spots occur. It can be seen that transport occurs only at quadruple points. The six QPs are labeled from 1 to 6. The inset in the left panel confirms that the transport spots occur as the  $(1,1,1)$  region closes. Similarly, the inset in the right panel, taken at a nearby  $C$  voltage, indicates that the transport spots occur as the  $(2,0,2)$  region closes. Table I lists the four degenerate electronic configurations at each QP.

The curved arrows in Fig. 4 indicate single-particle sequences involving only nearest neighbor events for transport (in analogy with the usual triple point sequential transport sequences in double quantum dots). Thus, for QP 1, an electron can be transferred through the device by the following sequence. Starting in  $(1,0,1)$ , an electron enters the left dot and transfers from dot to dot, exiting the right dot. Such a process requires all four configurations  $(1,0,1)$ ,  $(2,0,1)$ ,  $(1,1,1)$ , and  $(1,0,2)$ . In a similar fashion, for QP 6, hole transport occurs from right to left by going through the sequence  $(2,1,2)$ ,  $(2,1,1)$ ,  $(2,0,2)$ , and  $(1,1,2)$ .<sup>21</sup>

For QPs 2 and 5, the equivalent sequences are slightly more subtle. The sequence for QP 2, for example, starts with  $(1,0,2)$ . An electron is added to the left dot from the left lead to reach  $(2,0,2)$ . Then the electron from

the right dot escapes to the right lead to give (2,0,1), which gives rise to a net current. The system returns to the initial configuration via the (1,1,1) state. Note that the current carrying sequences for QPs 1, 2, 5, and 6 all correspond to a simple closed curve passing through the relevant four degenerate configurations similar to that at triple points in double quantum dots. These curves are drawn in the left and right panels in Fig. 4. In contrast, the sequences for QPs 3 and 4 differ from all the others, as their trajectories describe figures of eight, shown in the central panel of Fig. 4. For QP 3, we start with (1,0,2). An electron hops into the left dot from the left lead to reach (2,0,2). Then, a charge transfer occurs between the left and center dots to reach (1,1,2), and an electron from the right dot hops off to the right lead to get (1,1,1) and produce net current flow. Finally, a charge transfer from the center dot to the right dot occurs to restore the (1,0,2) configuration. Likewise, a similar process occurs for QP 4.

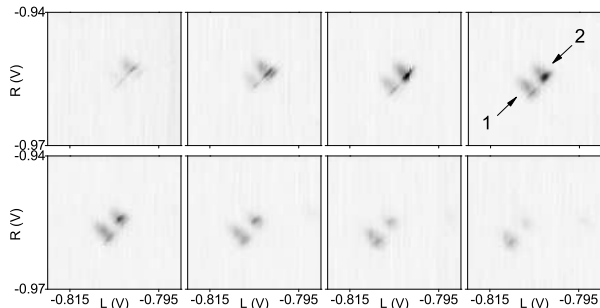


FIG. 3:  $C$  gate voltage dependence of DC current through the TQD in the R-L voltage plane near QPs 1 and 2 at  $V_{ds}=0.1$  mV.  $C$  goes from -0.218 V to -0.2165 V in the 1<sup>st</sup> row and from -0.216 V to -0.2145 V in the 2<sup>nd</sup> row. The greyscale from white to black corresponds to a current range of 730 fA.

In order to gain further understanding of the  $C$  gate evolution, we turn to using the equivalent circuit model<sup>13,15</sup> to identify where QPs occur within stability diagram. This model allows us to first calculate the energy of the TQD,  $E_{TQD}$ , for each of the eight relevant electronic configuration between (1,0,1) and (2,1,2) and everywhere in the 3D voltage space.  $E_{TQD}$  contains three terms: the charging energy for the electrons on each one of the three dots; the mutual capacitive energy for electrons on different dots; and the potential energy from the gate voltages.

To perform realistic calculations, we make assumptions about the relative sizes of the single electron charging energies, the mutual capacitive energies for electrons on different dots, and the gate-dot capacitances  $C_{gate,dot}$ . The mutual capacitive energy between adjacent (outer) dots is taken as 0.1 (0.01) times the charging energy.  $C_{gate,dot}$  are taken such that  $C_{L,C}=0.6C_{L,L}$ ,  $C_{L,R}=0.4C_{L,L}$ , and the rest of the capacitance matrix follows by symmetry.

In order to visualize the 3D stability diagram for the 8 electronic configurations between (1,0,1) and (2,1,2),

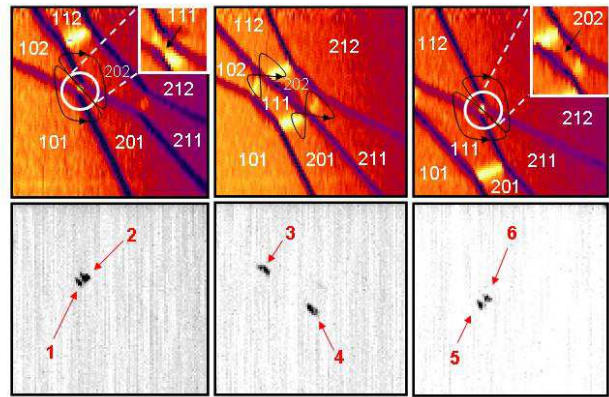


FIG. 4: (Color online.) Charge detection transconductance and DC transport reproduced from Fig. 2. The values of  $C$  in the left, middle, and right panels are -0.222 V, -0.216 V, and -0.208 V, respectively. The charge detection transconductance data are plotted with an arbitrary unit colorscale (dark blue is low, orange is medium, and yellow is high). The electronic configurations are indicated. The insets in the left and right panels are from  $C=-0.220$  V and -0.214 V, respectively. Arrows indicate sequences for current flow.

QP	Configurations	$n \times N$
1	(1,0,1) (1,1,1) (1,0,2) (2,0,1)	$1 \times 2$ and $3 \times 3$
2	(1,1,1) (1,0,2) (2,0,1) (2,0,2)	$3 \times 3$ and $1 \times 4$
3	(1,1,1) (1,1,2) (1,0,2) (2,0,2)	$2 \times 3$ and $2 \times 4$
4	(1,1,1) (2,0,1) (2,1,1) (2,0,2)	$2 \times 3$ and $2 \times 4$
5	(1,1,1) (1,1,2) (2,1,1) (2,0,2)	$1 \times 3$ and $3 \times 4$
6	(1,1,2) (2,1,1) (2,0,2) (2,1,2)	$3 \times 4$ and $1 \times 5$

TABLE I: Degenerate electronic configurations for the six QPs when adding one electron to the three quantum dots from (1,0,1) to (2,1,2). The number of configurations  $n$  with a given total electron number  $N$  are also indicated as  $n \times N$ .

one needs to find the location of several planes; namely, the planes where an electron is added to left dot; the planes where an electron is added to the right dot; the planes where an electron is added to the center dot; the planes where an electron is transferred between two dots; and the plane where the QCA effect occurs between the (1,1,1) and (2,0,2) configurations. The latter plane is a mixed plane where the addition of an electron and the charge transfer occur simultaneously.

All the planes that involve a change in the total number of electrons (i.e. including the QCA plane) are found by locating points in the 3D voltage space where  $E_{TQD}(N_L, N_C, N_R)$  is degenerate for two configurations (also requiring the two configurations to be the lowest energy states of the system). For the charge transfer planes, we require that the electrochemical potential  $\mu(N_L, N_C, N_R)$  of two configurations be equal (also requiring that the two con-

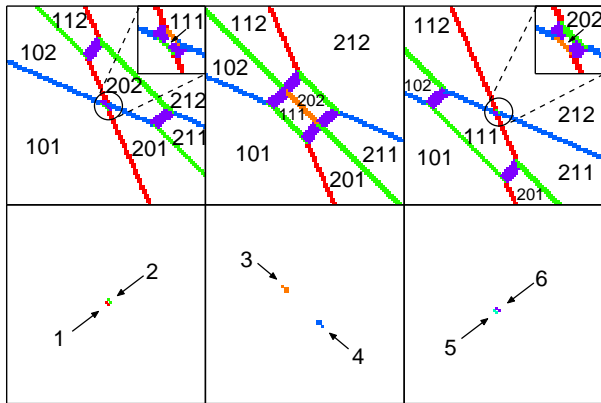


FIG. 5: (Color online.) 2D cuts from the calculated 3D stability diagram and QPs with increasing center plunger gate voltage from left to right. (top row) Stability diagrams, where red [green] [blue] lines correspond to adding an electron to the left [center] [right] dot, purple lines correspond to charge transfers, and the orange line corresponds to the QCA effect. Insets are zooms at values of  $C$  slightly off from the QP. (bottom row) The six QPs found from the model: 1 (red), 2 (green), 3 (orange), 4 (blue), 5 (turquoise), and 6 (purple).

figurations be the lowest energy states of the system). We define  $\mu(N_L, N_C, N_R) = E_{\text{TQD}}(N_L, N_C, N_R) -$

$E_{\text{TQD}}(N_L + N_C + N_R - 1)$ , where the last term is evaluated in the ground state of the  $N_L + N_C + N_R - 1$  configuration subspace. The calculated 3D stability diagrams are shown in the top row of Fig. 5.

The QPs are part of the stability diagram, as, by definition, they occur wherever the value of  $E_{\text{TQD}}$  is the same for four different electronic configurations. We use the equivalent circuit model to find where this four-fold degeneracy occurs. The results are drawn in the bottom row of Fig. 5 for the same  $C$  gate voltages as in the top row. The six QPs revealed numerically are comparable to the measurements of Figs. 2 to 4.

In conclusion, we have studied the interplay between transport and the 3D stability diagram of a triple quantum dot circuit in the regime with the electron configurations between  $(1,0,1)$  and  $(2,1,2)$ , relevant for spin qubits. We have found that transport occurs only at each of six quadruple points. The six quadruple points are consistent with a simple equivalent circuit model. Understanding of this interplay is important for quantum information experiments requiring transport through triple quantum dot circuits.

We thank D.G. Austing, P. Hawrylak, and C.Y. Hsieh for discussions. A.S.S. acknowledges funding from NSERC Grant No. 170844-05. A.S.S. and A.K. acknowledge funding from CIFAR. G.G. acknowledges funding from the NRC-CNRS collaboration.

\* Electronic address: Ghislain.Granger@nrc.ca

- <sup>1</sup> R. Hanson, L. P. Kouwenhoven, J. R. Petta, S. Tarucha, L. M. K. Vandersypen, *Reviews of Modern Physics*, **79**, 1217 (2007).
- <sup>2</sup> M. Pioro-Ladrière, T. Obata, Y. Tokura, Y.-S. Shin, T. Kubo, K. Yoshida, T. Taniyama, and S. Tarucha, *Nature Phys.* **4**, 776 (2008).
- <sup>3</sup> H. Bluhm, S. Foletti, I. Neder, M. Rudner, D. Mahalu, V. Umansky, and A. Yacoby, arXiv:1005.2995v1 and references therein.
- <sup>4</sup> L. Gaudreau, A. Kam, G. Granger, S.A. Studenikin, P. Zawadzki, and A.S. Sachrajda, *App. Phys. Lett.* **95**, 193101 (2009).
- <sup>5</sup> T. Tanamoto, *Phys. Rev. A* **61**, 022305 (2000).
- <sup>6</sup> D. Loss and D.P. DiVincenzo, *Phys. Rev. A* **57**, 120 (1998).
- <sup>7</sup> D.S. Saraga and D. Loss, *Phys. Rev. Lett.* **90**, 166803 (2003).
- <sup>8</sup> M. Busl, R. Sánchez, and G. Platero, *Phys. Rev. B* **81**, 121306(R) (2010).
- <sup>9</sup> A.D. Greentree, J.H. Cole, A.R. Hamilton, and L.C.L. Hollenberg, *Phys. Rev. B* **70**, 235317 (2004).
- <sup>10</sup> D.P. DiVincenzo, D. Bacon, J. Kempe, G. Burkard, and K. B. Whaley, *Nature* **408**, 339 (2000).
- <sup>11</sup> B. Michaelis, C. Emary, and C.W.J. Beenakker, *Europhys. Lett.* **73**, 677 (2006).
- <sup>12</sup> J. Fabian and U. Hohenester, *Phys. Rev. B* **72**, 201304(R) (2005).

- <sup>13</sup> L. Gaudreau, S.A. Studenikin, A.S. Sachrajda, P. Zawadzki, A. Kam, J. Lapointe, M. Korkusinski, and P. Hawrylak, *Phys. Rev. Lett.* **97**, 036807 (2006).
- <sup>14</sup> M.C. Rogge and R.J. Haug, *New J. of Phys.* **11**, 113037 (2009).
- <sup>15</sup> D. Schroer, A.D. Greentree, L. Gaudreau, K. Eberl, L.C.L. Hollenberg, J.P. Kotthaus, and S. Ludwig, *Phys. Rev. B* **76**, 075306 (2007).
- <sup>16</sup> L. Gaudreau, A.S. Sachrajda, S. Studenikin, A. Kam, F. Delgado, Y.P. Shim, M. Korkusinski, and P. Hawrylak, *Phys. Rev. B* **80**, 075415 (2009).
- <sup>17</sup> M. Field, C.G. Smith, M. Pepper, D.A. Ritchie, J.E.F. Frost, G.A.C Jones, and D.G. Hasko, *Phys. Rev. Lett.* **70**, 1311 (1993).
- <sup>18</sup> E.A. Laird, J.M. Taylor, D.P. DiVincenzo, C.M. Marcus, M.P. Hanson, and A.C. Gossard, arXiv:1005.0273v1.
- <sup>19</sup> The system can minimize its energy by spreading out the charge for the three electrons in  $(1,1,1)$ , but for four electrons the system minimizes its energy by going to separated pairs of electrons in  $(2,0,2)$ .
- <sup>20</sup> The exact values of  $C$  are slightly less negative here compared to the data in Figs. 2 and 4 because of a background charge jump between the experiments.
- <sup>21</sup> Equivalently, one can think about transport of an electron at QP 6 from left to right through a cyclic permutation of the hole transport sequence starting with  $(1,1,2)$ .